J Comput Electron
DOI 10.1007/s10825-015-0671-7

Suppressed and enhanced shot noise in one dimensional field-effect transistors

Giuseppe Iannaccone · Alessandro Betti · Gianluca Fiori

Abstract Landauer–Büttiker shot noise formula only considers the impact of Pauli exclusion principle on noise, but not the impact of Coulomb repulsion among carriers. A theory recently derived by the authors is able to include also the impact of Coulomb repulsion, and provides a computational methodology to obtain noise properties on a more complete physical basis. We review recent results from the application of this methodology with the use of in-house developed computational electronics tools. We show that in a one-dimensional FET, electrostatic repulsion among charge carriers in the channel can be responsible for strongly suppressed or enhanced shot noise with respect to the Poissonian Noise, or to the noise level provided by Landauer–Büttiker formula. This is very relevant for device and circuit design, since current semiconductor technology evolution has brought nanoscale FETs very close to the limit of one-dimensional FETs.

Keywords One-dimensional transistors · Carbon nanotube transistors · Shot noise

1 Introduction

Decades of Moore's law in action have shrunk the number of carriers in a Metal-Oxide-Semiconductor Field-Effect Transistors (MOSFETs) down to few units [1]. One side effects is that in a small ensemble fluctuations have a larger relative weight, and therefore the signal-to-noise ratio can rapidly degrade at a critical level for device operation.

G. Iannaccone (✉) · A. Betti · G. Fiori
Dipartimento di Ingegneria dell'Informazione, Università di Pisa, Pisa, Italy
e-mail: giuseppe.iannaccone@unipi.it

For this reason, electrical noise in nanoscale devices has attracted significant interest, with focus moving from diffusive mesoscopic conductors [2–6], to nanoscale [7–9] and on carbon-based electronic devices [10–14].

When carriers are highly correlated, either sub- or super-poissonian noise can be observed. In particular, noise enhancement has been observed in resonant tunneling diodes [15,16], due to the positive correlation between electrons tunneling into the quantum well caused by the interplay between the density of states in the well and electrostatics.

The impact of the electrostatic interaction on noise has been addressed by Büttiker and coworkers, with specific reference to the noise of a capacitor, i.e., by describing all electrostatic effects through a single capacitor [17,18]. However, in several cases of interest, such as evaluating the noise of a field-effect transistor, the assumption of a single potential in the conductor can be an oversimplification, and a more general approach is desired.

In this paper we discuss a more general methodology based on statistical Monte Carlo simulations with states randomly injected from the contacts [13,14] to evaluate shot noise suppression in (13,0) CNT-FETs and SNW-FETs [13,14]. In particular, we compare the noise power spectrum calculated by means of Monte Carlo simulations to that provided by the Landauer–Büttiker noise formula, i.e., considering only Pauli exclusion principle, in order to fully understand the effect of Coulomb repulsion on noise. We also compute the partition and the injection noise components, and highlight the importance of exchange interference noise contribution [14,19]. In addition, we compare shot noise and thermal noise and predict the effect of scaling of device length and oxide thickness on noise [13].

Then, we discuss a case in which the opposite effect takes place: shot noise enhancement in (25,0) CNT-FETs [20,21],

caused by the modulation of electron injection from the source due to the transfer of holes between the drain and the channel. We investigate the temperature and frequency ranges where the noise enhancement is detectable in experiments.

2 Theory and devices under study

We briefly report the main theoretical results, derived in [13, 14] with two different methods.

The noise current spectral density is experimentally obtained by measuring the time-dependent current over a long observation time, then by computing the Fourier transform of the autocorrelation function of the AC component of the current. The shot noise power spectrum is flat up to a frequency of the order of the inverse transit time, which is usually not observable in experiments, because at that frequency shot noise is completely masked by the noise of the measurement amplifier. For this reason, we are only interested in the flat region of the shot noise power spectrum, the so-called zero frequency shot noise.

The zero frequency noise spectrum is proportional to the variance of the current. We can exploit the ergodicity theorem in order not to perform time-dependent simulations, and instead compute the statistical variance of the current, which in turn depends on the statistical distribution of injected electrons from the contacts.

Let us consider a mesoscopic conductor connected to two reservoirs [source (S) and drain (D)], where electron states are populated according to their Fermi occupation factors (Fig. 1). For simplicity, we assume that the conductor is sufficiently short as to completely neglect inelastic scattering events. Thermalization occurs only in the reservoirs.

The statistical average $\langle I \rangle$ of the current I in the FET channel can be written as:

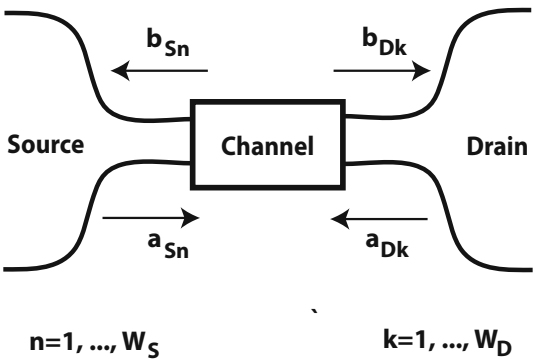

Fig. 1 Annihilation operators for ingoing (a_{Sm}, a_{Dn}) and outgoing electron states (b_{Sm}, b_{Dn}) in a two terminal scattering problem ($m = 1, \ldots, W_S$; $n = 1, \ldots, W_D$)

$$\begin{aligned}\langle I \rangle &= \frac{e}{h}\int dE\left\{\sum_{n\in S}\left\langle\left[\mathbf{t}^{\dagger}\mathbf{t}\right]_{nn}\sigma_{Sn}\right\rangle_s - \sum_{k\in D}\left\langle\left[\mathbf{t}'^{\dagger}\mathbf{t}'\right]_{kk}\sigma_{Dk}\right\rangle_s\right\} \\ &= \frac{e}{h}\int dE\left\{\sum_{n\in S}\left\langle\left[\tilde{\mathbf{t}}\right]_{S;nn}\sigma_{Sn}\right\rangle_s - \sum_{k\in D}\left\langle\left[\tilde{\mathbf{t}}\right]_{D;kk}\sigma_{Dk}\right\rangle_s\right\},\end{aligned} \tag{1}$$

where the e is the elementary charge, h is Planck's constant, and sums run over all quantum channels of the source and drain leads. Most importantly, $\sigma_{\alpha n}$ is the actual occupation factor of quantum channel n injected from reservoir α ($\alpha = S, D$), and therefore is either 0 or 1, its average being determined by Fermi Dirac statistics of reservoir α ($\langle\sigma_{\alpha n}\rangle = f_\alpha(E_n)$). We also can assume correlation is zero between occupation factors of different quantum channels.

The blocks $\mathbf{r}$ (size $W_S \times W_S$) and $\mathbf{t}'$ (size $W_S \times W_D$), are the reflection matrix at the source ($\mathbf{r}$) and the transmission matrix from drain to source ($\mathbf{t}'$), respectively, and are included in the (unitary) scattering matrix $\mathbf{s}$ as [22]:

$$\mathbf{s} = \begin{pmatrix} \mathbf{r} & \mathbf{t}' \\ \mathbf{t} & \mathbf{r}' \end{pmatrix}. \tag{2}$$

The dimensions of $\mathbf{s}$ are $(W_S + W_D) \times (W_S + W_D)$. Blocks $\mathbf{t}$ and $\mathbf{r}'$ in Eq. (2) are related to source-to-drain transmission and reflection back to the drain, respectively. In addition, $\left[\tilde{\mathbf{t}}\right]_{\alpha;lp} \equiv \left[\mathbf{t}^{\dagger}\mathbf{t}\right]_{lp}$ if $\alpha = S$ and $\left[\mathbf{t}'^{\dagger}\mathbf{t}'\right]_{lp}$ if $\alpha = D$ ($l, p \in \alpha$). It is easy to show that for a non-interacting channel, i.e. when occupancy of injected states does not affect transmission and reflection probabilities, Eq. (1) reduces to the two-terminal *Landauer's formula* [23]:

$$\langle I \rangle = \frac{e}{h}\int dE\,\mathrm{Tr}\left[\mathbf{t}^{\dagger}\mathbf{t}\right](f_S(E) - f_D(E)), \tag{3}$$

where the relation $\mathbf{s} = \mathbf{s}^{\mathbf{t}}$ has been exploited, so that $\mathbf{t}' = \mathbf{t}^{\mathbf{t}}$ and $\mathrm{Tr}\left[\mathbf{t}'^{\dagger}\mathbf{t}'\right] = \mathrm{Tr}\left[\mathbf{t}^{\dagger}\mathbf{t}\right]$. In general, we can observe that for an interacting channel Eq. (1) provides a different result with respect to Landauer's formula, because fluctuation of transmission probabilities induced by random injection in the device, is responsible for rectification of the current. The effect is often very small, but not always [13]. However, it cannot be captured by Landauer's formula, as other many-particle processes affecting device transport properties [24,25].

The power spectral density of shot noise at zero frequency, expressed as:

$$S(0) = \lim_{\nu\to 0}\frac{2}{\nu}var(I) = \lim_{\Delta E\to 0} 4\pi\hbar\frac{var(I)}{\Delta E}, \tag{4}$$

can be finally [13] written as

$$
\begin{aligned}
S(0) = &\left(\frac{e^2}{\pi\hbar}\right)\int dE \sum_{\alpha=S,D}\sum_{l\in\alpha}\left\langle [\tilde{\mathbf{t}}]_{\alpha;ll}\left(1-[\tilde{\mathbf{t}}]_{\alpha;ll}\right)\sigma_{\alpha l}\right\rangle_s \\
&-\left(\frac{e^2}{\pi\hbar}\right)\int dE \sum_{\alpha=S,D}\sum_{\substack{l,p\in\alpha \\ l\neq p}}\left\langle [\tilde{\mathbf{t}}]_{\alpha;lp}[\tilde{\mathbf{t}}]_{\alpha;pl}\,\sigma_{\alpha l}\sigma_{\alpha p}\right\rangle_s \\
&-2\left(\frac{e^2}{\pi\hbar}\right)\int dE \sum_{k\in D}\sum_{p\in S}\left\langle [\mathbf{t}'^{\dagger}\mathbf{r}]_{kp}\,[\mathbf{r}^{\dagger}\mathbf{t}']_{pk}\,\sigma_{Dk}\sigma_{Sp}\right\rangle_s \\
&+\frac{4\pi\hbar}{\Delta E}var\left\{\frac{e}{h}\int dE\left(\sum_{n\in S}[\tilde{\mathbf{t}}]_{S;nn}\sigma_{Sn}-\sum_{k\in D}[\tilde{\mathbf{t}}]_{D;kk}\sigma_{Dk}\right)\right\}.
\end{aligned}
\tag{5}
$$

Let us consider that case in which transmission and reflection matrices do not depend on random occupation numbers of injected states, i.e. a non fluctuating potential profile is imposed along the channel, By exploiting the reversal time symmetry ($\mathbf{s} = \mathbf{s}^{\mathbf{t}}$, so that $\mathbf{t}' = \mathbf{t}^{\mathbf{t}}$), the unitarity of the scattering matrix, Eq. (5) reduces to:

$$
\begin{aligned}
S(0) = &\frac{2e^2}{\pi\hbar}\int dE\left\{[f_S(1-f_S)+f_D(1-f_D)]\,\mathrm{Tr}\left[\mathbf{t}^{\dagger}\mathbf{t}\mathbf{t}^{\dagger}\mathbf{t}\right]\right. \\
&+[f_S(1-f_D)+f_D(1-f_S)] \\
&\left.\times\left(\mathrm{Tr}\left[\mathbf{t}^{\dagger}\mathbf{t}\right]-\mathrm{Tr}\left[\mathbf{t}^{\dagger}\mathbf{t}\mathbf{t}^{\dagger}\mathbf{t}\right]\right)\right\},
\end{aligned}
\tag{6}
$$

which is the well-known *Landauer–Büttiker noise formula* [26].

We can use this result to study the behavior of shot noise in quasi-1D channel of CNT-FETs and SNW-FETs with identical reservoirs (Fig. 2). We consider a (13,0) CNT embedded in SiO_2 with oxide thickness equal to 1 nm, an undoped channel of 10 nm and n-doped CNT extensions 10 nm long, with a molar fraction $f = 5\times10^{-3}$. The SNW-FET has an oxide thickness (t_{ox}) equal to 1 nm and the channel length (L) is 10 nm. The channel is undoped and the source and drain extensions (10 nm long) are doped with $N_D = 10^{20}$ cm^{-3}. The device cross section is 4×4 nm^2.

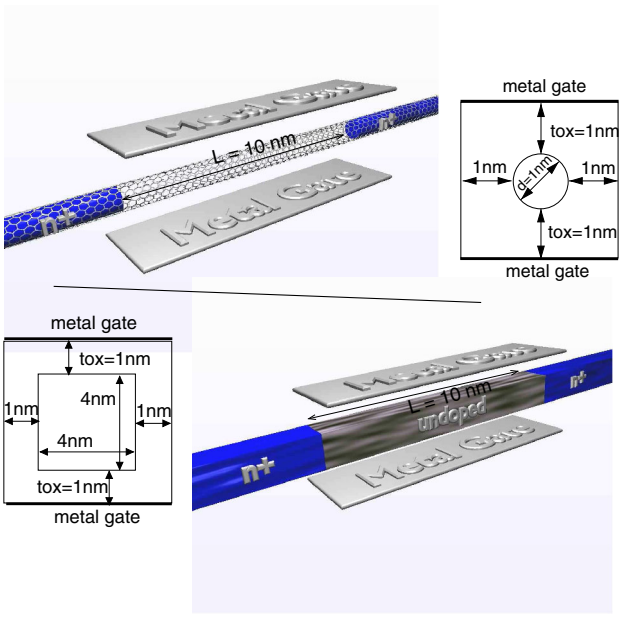

Fig. 2 3-D structures and transversal cross sections of the simulated CNT (*top*) and SNW-FETs (*bottom*). From Ref. [13]

In order to properly include the effect of Coulomb interaction, we perform self-consistent simulations of the 3D Poisson equation, coupled with the Schrödinger equation with open boundary conditions, within the NEGF formalism, which has been implemented in our in-house open source simulator *NanoTCAD ViDES* [27].

From a numerical point of view, a p_z-orbital tight-binding Hamiltonian has been assumed for CNTs [28,29], whereas an effective mass approximation has been considered for SNWs [30,31] by means of an adiabatic decoupling in a set of two-dimensional equations in the transversal plane and in a set of one-dimensional equations in the longitudinal direction for each 1D subband. For both devices, we have developed a quantum ballistic transport model with semi-infinite extensions at their ends. A mode space approach has been adopted, since only the lowest subbands take part to transport. In particular, we have verified that four modes are enough to compute the mean current both in the ohmic and saturation regions. All calculations have been performed at room temperature ($T = 300$ K).

We call SC simulations those self-consistent simulations in which the occupation factor of all quantum channels is the Fermi-Dirac occupation factor. On the other hand, in order to model the stochastic injection of electrons from the reservoirs, we have performed self-consistent Monte Carlo (SC-MC) simulations taking into account an ensemble of many electron states, i.e. an ensemble of random configurations of injected electron states, from both contacts [13,14]. In this case the occupation factors or each quantum channel are randomly 0 or 1, with average provided by Fermi-Dirac statistics. In our case, we have verified that an ensemble of 500 random configurations represents a good trade-off between computational cost and accuracy.

3 DC characteristics

In Fig. 3, the transfer characteristics for different drain-to-source biases V_{DS} computed performing SC and SC-MC simulations are plotted as a function of the gate overdrive $V_{GS} - V_{th}$ in the logarithmic scale, both for CNT and SNW devices. In particular the threshold voltage V_{th} for the CNT-FET at $V_{DS} = 0.05$ V and 0.5 V is 0.43 V, whereas we obtain $V_{th} = 0.13$ V for $V_{DS} = 0.05$ V and 0.5 V for the SNW-FET. As can be noted, SC and SC-MC simulations give practically the same results for CNT-FET, except in the subthreshold region where an interesting rectifying effect of

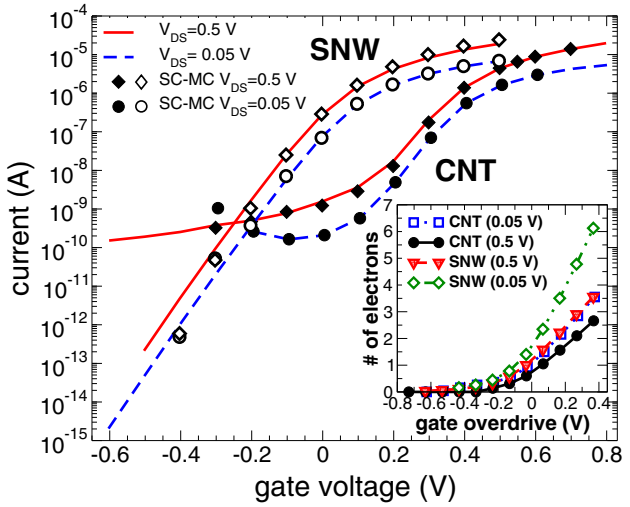

Fig. 3 Transfer characteristics computed for V_{DS} = 0.5 and 0.05 V, obtained by SC-MC and SC simulations, for CNT and SNW-FET. *Full dots* refer to CNT, *empty dots* to SNW. *Inset* average number of electrons in CNT-FETs and SNW-FETs channel, evaluated for V_{DS} = 0.5 and 0.05 V. From Ref. [13]

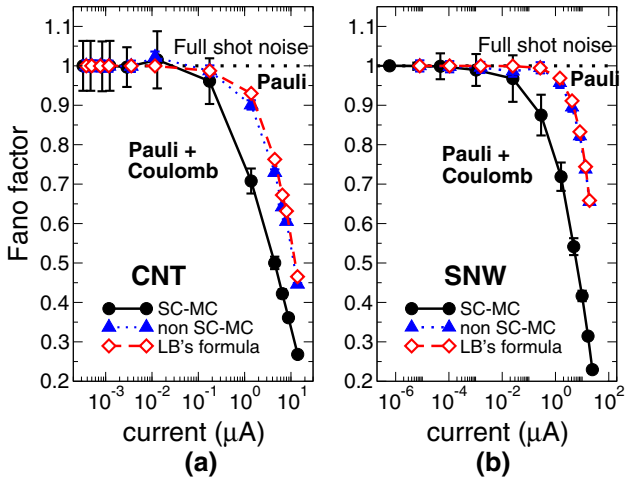

Fig. 4 Fano factor as a function of the drain current $\langle I \rangle$ for **a** CNT- and **b** SNW-FETs for V_{DS} = 0.5 V. *Solid line* refers to the Fano factor F obtained by means of SC-MC simulations, *dashed line* (*diamonds*) applying Eq. (6) and *dotted line* (*triangles*) by means of non SC-MC simulations. From Ref. [13]

the statistics emerges in the Monte Carlo simulations for a drain-to-source bias $V_{DS} = 0.5$ V.

Instead, the rectifying effect is larger for SNW-FET, differences up to 30 % between the drain current $\langle I \rangle$ computed by means of SC-MC and SC simulations can be also observed in the above threshold regime. In particular, for a gate voltage $V_{GS} = 0.5$ V and a drain-to-source voltage $V_{DS} = 0.5$ V, the drain current $\langle I \rangle$ holds 2.42×10^{-5} A applying Eq. (1), and 1.89×10^{-5} A applying Landauer's formula (3). Current in the CNT-FET transfer characteristics increases for negative gate voltages due to the interband tunneling. Indeed, the larger the negative gate voltage, the higher the number of electrons that tunnel from bound states in the valence band to the drain, leaving positive charge in the channel, which eventually lowers the barrier and increases the off current [32].

In the inset of Fig. 3 the average number of electrons inside the channel of a CNT and SNW-FET for two different biases V_{DS} = 0.5 V and 0.05 V is shown. As can be seen, only very few electrons contribute to transport at any give instant, which requires us to attently evaluate the sensitivity of such devices to charge fluctuations: the smaller the drain-to-source voltage, the larger the average number of electrons in the channel, since, for low V_{DS}, carriers are injected from both contacts.

4 Shot noise suppression in (13,0) CNT-FETs and SNW-FETs

Let us now focus our attention on the Fano factor F, defined as the ratio of the computed noise power spectral density $S(0)$ to the full shot noise $2e\langle I \rangle$, $F = S(0)/(2e\langle I \rangle)$. In Fig. 4, the Fano factor for both CNT-FETs and SNW-FETs is shown for V_{DS} = 0.5 V as a function of drain-to-source current $\langle I \rangle$.

Let us discuss separately the effects of Pauli exclusion alone and concurrent Pauli and Coulomb interactions. Triangles in Fig. 4 refer to F computed by means of non SC-MC simulations on 10^4 samples, while diamonds to results obtained by means of Landauer–Büttiker's formula, applying Eq. (6). As expected the two approaches give the same results for both structures. Solid lines refer to $S(0)$ computed by means of Eqs. (5) and (4) and SC-MC simulations, i.e. Pauli and Coulomb interactions simultaneously taken into account.

In the sub-threshold regime ($\langle I \rangle < 10^{-9}$ A, $V_{GS} - V_{th} <$ -0.2 V), drain current noise is very close to the full shot noise, since electron-electron correlations are negligible due to the very small amount of mobile charge in the channel.

From the point of view of Eq. (6), for energies larger than the top of the barrier, we have $f_D(E) \ll f_S(E) \ll 1$ and the integrand in (6) reduces to $\mathrm{Tr}\left[\mathbf{t}^\dagger \mathbf{t}(E)\right] f_S(E)$. Instead, for energies smaller than the high potential profile along the channel, $\left[\mathbf{t}^\dagger \mathbf{t}(E)\right]_{nm} \ll 1 \; \forall n,\, m \in S$, so that we can neglect $\mathrm{Tr}\left[\mathbf{t}^\dagger \mathbf{t}\, \mathbf{t}^\dagger \mathbf{t}\right]$ in (6), with respect to $\mathrm{Tr}\left[\mathbf{t}^\dagger \mathbf{t}\right]$. Since $f_D(E) \ll f_S(E)$, the integrand in (6) still reduces to $\mathrm{Tr}\left[\mathbf{t}^\dagger \mathbf{t}(E)\right] f_S(E)$. The Fano factor then becomes

$$F = \frac{S(0)}{2e\langle I \rangle} \approx \frac{\frac{2e^2}{\pi\hbar} \int dE\, \mathrm{Tr}\left[\mathbf{t}^\dagger \mathbf{t}(E)\right] f_S(E)}{2e\frac{e}{\pi\hbar} \int dE\, \mathrm{Tr}\left[\mathbf{t}^\dagger \mathbf{t}(E)\right] f_S(E)} = 1 \qquad (7)$$

In the strong inversion regime instead ($\langle I \rangle > 10^{-6}$ A, $V_{GS} - V_{th} > 0$ V), the noise is strongly suppressed with respect to the full shot value. In particular for a SNW-FET, at $\langle I \rangle \approx 2.4 \times 10^{-5}$ A ($V_{GS} - V_{th} \approx 0.4$ V), combined Pauli and Coulomb interactions suppress shot noise down to 22 % of the

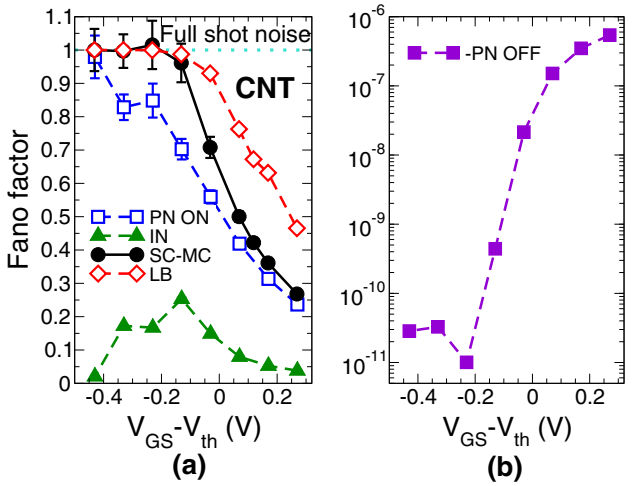

Fig. 5 Contributions to the Fano factor in a CNT-FET of the on-diagonal and off-diagonal partition noise and of the injection noise (respectively on-diagonal and off-diagonal part of the first three terms, and fourth term in Eq. (5)) as a function of the gate overdrive $V_{GS} - V_{th}$ for a drain-to-source bias $V_{DS} = 0.5$ V. **a** The on-diagonal partition (PN ON, *open squares*), the injection (IN, *solid triangles up*) and the full noise (*solid circles*) computed by means of SC-MC simulations are shown. The Fano factor computed by exploiting Landauer–Büttiker's formula (6) and SC simulations (*open diamonds*) is also shown. **b** Off-diagonal partition noise contribution (PN OFF) to F due to correlation between transmitted states and between transmitted and reflected states. From Ref. [14]

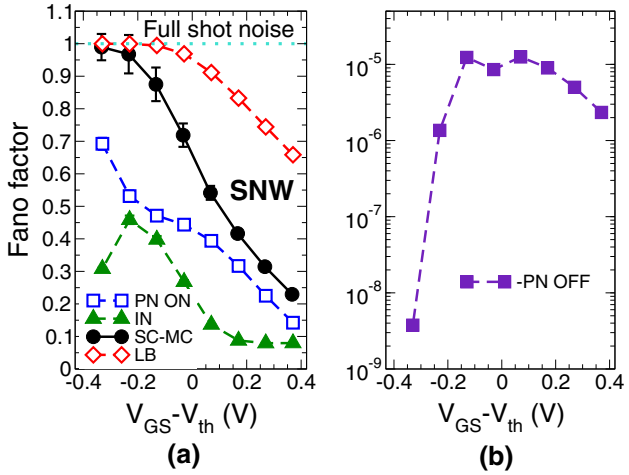

Fig. 6 Contributions to the Fano factor in a SNW-FET of the on-diagonal and off-diagonal partition noise and of the injection noise, obtained for $V_{DS} = 0.5$ V, as a function of the gate overdrive $V_{GS} - V_{th}$ in a SNW-FET. In **a** the on-diagonal partition, the injection and the full noise computed by means of SC-MC simulations (both Pauli and Coulomb interactions taken into account) are shown together with results obtained by means of Eq. (6). **b** Off-diagonal partition noise due to correlation between transmitted states and between transmitted and reflected states. From Ref. [14]

full shot noise value, with a significant reduction with respect to the value predicted without including space charge effects as in Ref. [33], while for CNT-FET the Fano factor is equal to 0.27 at $\langle I \rangle \approx 1.4 \times 10^{-5}$ A ($V_{GS} - V_{th} \approx 0.3$ V). Indeed, an injected electron tends to increase the potential barrier along the channel, leading to a reduction of the space charge and to a suppression of charge fluctuation. Let us stress that an SC-MC simulation exploiting Eq. (5) is mandatory for a quantitative evaluation of noise. Indeed, by only considering Pauli exclusion principle through formula (6), one would have overestimated shot noise by 180 % for SNW-FET ($\langle I \rangle \approx 2.4 \times 10^{-5}$ A, $V_{GS} - V_{th} \approx 0.4$ V) and by 70 % for CNT-FET ($\langle I \rangle \approx 1.4 \times 10^{-5}$ A, $V_{GS} - V_{th} \approx 0.3$ V) [12,13].

Now let us focus our attention on the partition PN (first three terms in Eq. (5)) and injection IN (fourth term in Eq. (5)) noise components of the Fano factor F. In Figs. 5 and 6 the contributions to F of PN and IN noises are shown, as a function of the gate overdrive $V_{GS} - V_{th}$ for a drain-to-source bias $V_{DS} = 0.5$ V for CNT-FETs and SNW-FETs, respectively: results have been obtained by means of SC-MC simulations. In particular, Figs. 5a and 6a refer to the on-diagonal contribution to the partition noise (solid circles), to the injection noise (open triangles up) and to the complete Fano factor (open circles) obtained by means of Eq. (5), i.e. Pauli and Coulomb interactions simultaneously considered. We present also the Fano factor (solid triangles down) computed by applying Eq. (6) on the self-consistent potential profile, i.e. when only Pauli exclusion principle is included. In Figs. 5b and 6b we show the contribution of the off-diagonal partition noise to F, which provides a measure of mode-mixing and of exchange interference effects [14,19].

As shown in Fig. 5a, the dominant noise source in ballistic CNT-FETs is the on-diagonal partition noise and the noise due to the intrinsic thermal agitations of charge carriers in the contacts (injection noise), which is at most the 36 % of the partition noise ($V_{GS} - V_{th} \approx -0.1$ V). Nearly identical results are shown for SNW-FETs, with the exception of a stronger contribution given by the injection noise, up to the 86 % of the on-diagonal partition term ($V_{GS} - V_{th} \approx -0.2$ V). Moreover, the behavior of the two noise components, as a function of $V_{GS} - V_{th}$, is very similar for both CNT- and SNW-FETs: F tends to 1 in the subthreshold regime, while in strong inversion regime shot noise is strongly suppressed.

It is also interesting to observe that the off-diagonal contribution to partition noise, due to exchange correlations between transmitted states and between transmitted and reflected states, has a strong dependence on the height of the potential profile along the channel (variation of 5 orders of magnitude for CNT-FETs) and is negligible for quasi one-dimensional FETs. In particular, for CNT-FETs such term is at most 5 orders of magnitude smaller than the on-diagonal partition noise or injection noise in the strong inversion regime ($V_{GS} - V_{th} \approx 0.3$ V), while in the subthreshold regime its magnitude still reduces (about 10^{-11} for

$V_{GS} - V_{th} \approx$ -0.4 V). For SNW-FETs we have obtained similar results: the off-diagonal partition noise is indeed at most 5 orders of magnitude smaller than the other two contributions.

In such conditions, transmission occurs only along separate quantum channels and an uncoupled mode approach is also accurate. Indeed, off-diagonal partition noise provides an interesting information on the strength of the mode-coupling which, as already seen, is very small. In particular, neglecting this term, results obtained from Eq. (5) can be recovered as well.

4.1 On the importance of exchange interference effects on current fluctuations

In the previous discussion, carriers from different quantum channels do not interfere. However, since we deal with a many indistinguishable particle system, such effects can come into play. To this purpose, we investigate in more detail two examples in which exchange pairings, that include also exchange interference effects, give a non negligible contribution to drain current noise. In the past exchange interference effects have been already predicted for example in ballistic conductor with an elastic scattering center in the channel [34], in diffusive four-terminal conductors of arbitrary shape [3] and in quantum dot in the quantum Hall regime [35], connected to two leads via quantum point contacts.

In the first case we discuss, mode-mixing does not appear, i.e. the non-diagonal elements of the matrices $\mathbf{t}^{\dagger}\mathbf{t}$ and $\mathbf{t}'^{\dagger}\mathbf{r}$ are negligible with respect to the diagonal ones. Since the off-diagonal partition noise is negligible and since in the third term in Eq. (5) only contributions with indices $l = n = k = p$ survive, exchange interference effects do not contribute to electrical noise. We consider a CNT-FET at low bias condition: $V_{DS} = 50$ mV. In Fig. 7a the on-diagonal partition noise, the injection noise and correlations due to the off-diagonal partition noise, evaluated performing statistical SC-MC simulations, are shown. In this case, on-diagonal correlations between transmitted and reflected states in the source lead (in the same quantum channel) extremely affect noise. Indeed, at the energies at which reflection events in the source lead are allowed, also electrons coming from D can be transmitted into the injecting contact S, since the corresponding energy states in D are occupied and the barrier height is small. Instead the exchange correlations represented by the off-diagonal partition noise are negligible, since they are at least 5 order of magnitude smaller than the other three terms in Eq. (5). Note that the noise enhancement obtained both in the inversion and subthreshold regimes is due to the fact that at low bias the current $\langle I \rangle$ becomes small, while the noise power spectrum $S(0)$ tends to a finite value, because of the thermal noise contribution.

Let now consider the situation in which modes are coupled and exchange interference effects, through the off-diagonal

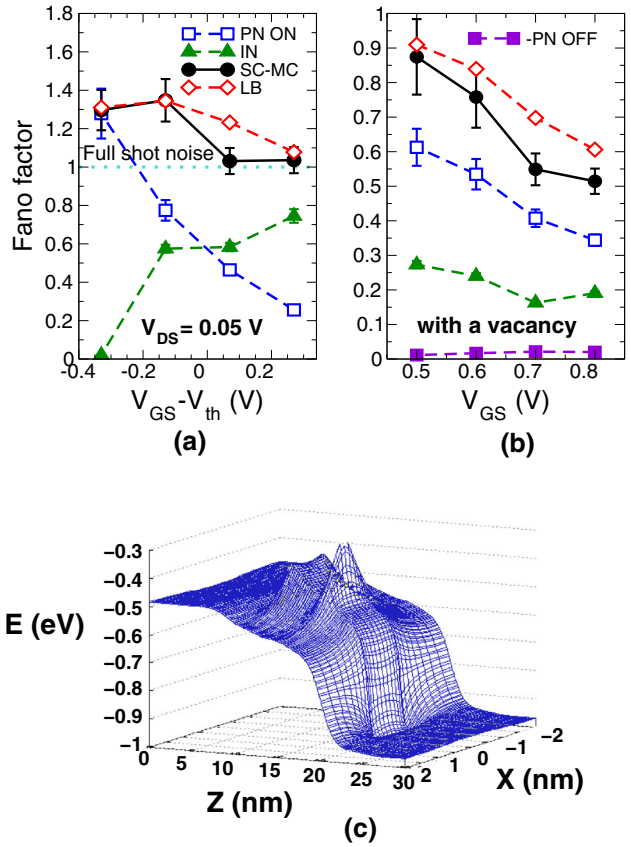

Fig. 7 **a** Contributions to the Fano factor F by the on-diagonal partition noise (*open squares*), and the injection noise (*solid triangles up*) as a function of the gate overdrive $V_{GS} - V_{th}$, for a drain-to-source bias $V_{DS} = 50$ mV. The simulated device is a CNT-FET. The full noise computed by means of SC-MC simulations (*solid circles*, both Pauli and Coulomb interactions taken into account) and applying Eq. (6) (*open diamonds*, only Pauli exclusion considered) is also shown. **b** Contributions to F by the on-diagonal and off-diagonal partition noise and by the injection noise (exploiting Eq. (5)) as a function of the gate overdrive for a CNT-FET with a vacancy in a site at the center of the channel. The drain-to-source bias is 0.5 V. **c** Self-consistent midgap potential obtained by using the Fermi statistics for a gate voltage $V_{GS} = 0.7$ V and a bias $V_{DS} = 0.5$ V. Z is the transport direction along the channel, X is a transversal direction. The simulated device is the same of (**b**). From Ref. [14]

partition noise, contribute to drain current fluctuations. We consider the interesting case in which a vacancy, i.e. a missing carbon atom, is placed at the center of the channel of a (13,0) CNT-FET. From a numerical point of view, this defect can be modelled by introducing a strong repulsive potential (i.e. +8 eV, much larger than the energy gap of a (13,0) CNT: $E_{gap} \approx$ 0.75 eV) in correspondence of such site, thus acting as a barrier for transmission in the middle of the channel (Fig. 7c).

In Fig. 7b the three noise sources in Eq. (5) (on- and off-diagonal partition noise, injection noise) are plotted as a function of the gate voltage V_{GS} in the above threshold regime for $V_{DS} = 0.5$ V, along with the full Fano factor computed performing SC and SC-MC simulations. Remarkably,

in this case a mode space approach taking into account all modes (i.e. 13) is mandatory in order to reproduce all correlation effects on noise. As can be seen, off-diagonal exchange correlations gives rise to a not negligible correction to the Fano factor [14] (≈ 4 % of the full Fano factor at $V_{GS} = 0.8$ V). We observe that such correlations are only established between transmitted electrons states (second term in Eq. (5)), while correlations between reflected and transmitted electron states (third term in Eq. (5)) are negligible since almost all electrons injected from the receiving contact D are reflected back because of the high bias condition. In this section we have assumed phase-coherent quantum transport at room temperature. Our tools cannot include electron-phonon interaction, that at room temperature may play a role even in nanoscale devices. Ref. [36] has considered the effect of electron-phonon scattering and has neglected Coulomb interaction: they find that electron-phonon scattering increases shot noise in the above threshold regime, due to the broadening of the energy range of electron states contributing to transport.

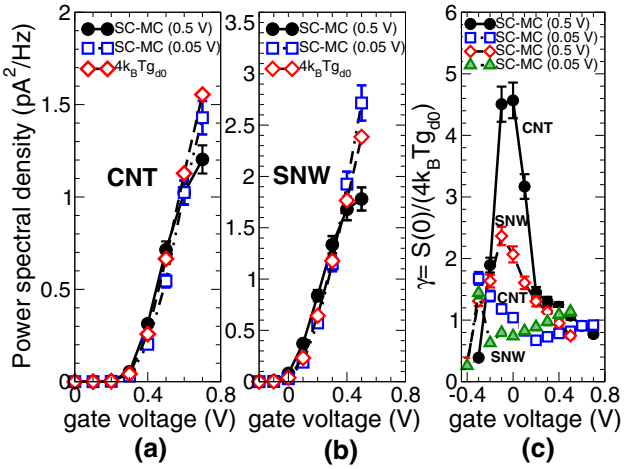

Fig. 8 **a** Noise power spectral density obtained by SC-MC simulations and thermal noise spectral density as functions of the gate voltage for **a** CNT-FETs and **b** SNW-FETs: the considered drain-to-source biases ($V_{DS} = 0.5$, 0.05 V) are shown in *brackets*; **c** ratio between the noise power obtained by SC-MC simulations and the thermal noise density as a function of the gate voltage. g_{d0} is the conductance evaluated for $V_{DS} = 0$ V: $g_{d0} = \left(\frac{\partial \langle I \rangle}{\partial V_{DS}}\right)_{V_{DS}=0}$. From Ref. [13]

4.2 Shot noise versus thermal channel noise

According to the classical approach for the formulation of drain current noise, channel noise is tipically described in terms of a "modified" thermal noise, as $S(0) = \gamma S_T$, where $S_T = 4K_B T g_{d0}$ is the thermal noise power spectrum at zero drain-to-source bias V_{DS}, k_B is the Boltzmann constant, γ is a correction parameter and $g_{d0} = (\partial \langle I \rangle / \partial V_{DS})_{V_{DS}=0}$ is the source-to-drain conductance at zero V_{DS}.

Although the classical formulation accurately predicts drain current noise in long channel MOSFETs, where γ is equal to 1 in the ohmic region and 2/3 in saturation [37], it underestimates noise in short channel devices. In particular, experimental evidences [38] of an excess noise in short channel MOSFET have been explained in terms of the limited number of scattering events inside the channel which is uneffective in suppressing the non-equilibrium noise component [39], or in terms of a revised classical formulation by considering short channel effects, such as the carrier heating effect above the lattice temperature [40].

Actually, it can clearly be seen that non equilibrium transport easily provides $\gamma > 1$ and that the cause of $\gamma > 1$ is simply due to the fact that channel noise can be more properly interpreted as shot noise. For example, in the particular case of ballistic transport considered here, we can plot γ as $S(0)/S_T$ as a function of the gate voltage in Fig. 8c. As can be seen, values of γ larger than 1 can be easily observed in weak and strong inversion. The strange behavior of γ as a function of the gate voltage is simply due to the fact that one uses an inadequate model (thermal noise) corrected with the γ parameter to describe a qualitatively different type of noise, i.e. shot noise.

4.3 Effect of scaling on noise

Let us now discuss the effect of scaling on noise, focusing our attention on a (13,0) CNT-FET. One would expect that an increase of the oxide thickness would reduce the screening induced by the metallic gate, so that the Coulomb interaction would be expected to produce a larger noise suppression. For example, in the limit of a multimode ballistic conductor without a gate contact, significantly suppression of about two order of magnitude with respect to the full shot value has been shown by Bulashenko et al [41].

However, Ref. [41] exploits a semiclassical approach assuming a large number of modes and the conservation of transversal momentum, i.e. the role of the transversal electric field induced by the gate voltage is completely neglected. In our case only four modes contribute to transport, while the top and bottom gates of the simulated devices partially screen the electrostatic repulsion induced by the space charge in the channel on each injected electron, so that a smaller noise suppression than the one achieved in Ref. [41] can be expected.

The Fano factor as a function of the average number of electrons inside the channel for unit length, computed by means of SC simulation and applying Eq. (6), for three CNTs with different oxide thickness t_{ox} and channel length L is shown in Fig. 9a: it shows results for CNT with t_{ox}= 1 nm, L= 6 nm (A), CNT with t_{ox} = 1 nm, L = 10 nm (B), and CNT with t_{ox} = 2 nm, L = 10 nm (C). Fig. 9b shows the Fano factor computed by performing SC-MC simulations and applying Eqs. (5) and (4). As can be seen, if the Fano factor is plotted as a function of the number of electrons per unit length, as

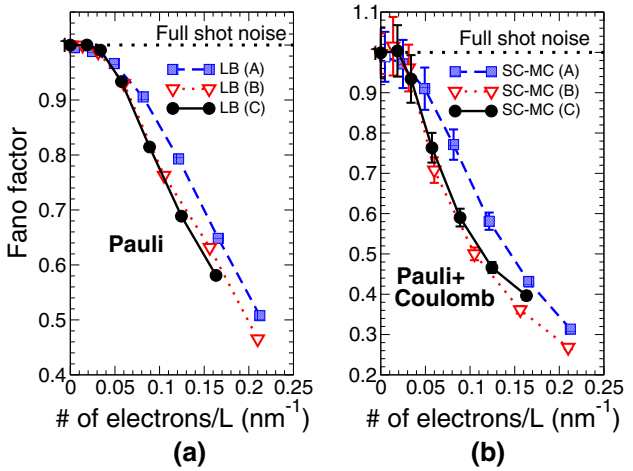

Fig. 9 Fano factor as a function of the average number of electrons inside the channel per unit length for three different (13,0) CNT-FETs: (*A*) $t_{ox} = 1$ nm, $L = 6$ nm, (*B*) $t_{ox} = 1$ nm, $L = 10$ nm and (*C*) $t_{ox} = 2$ nm, $L = 10$ nm. In **a** only the effect of the Pauli principle is shown [Eq. (6)]; in **b** the effect of both Pauli and Coulomb interactions is considered. The drain-to-source bias V_{DS} is 0.5 V. From Ref. [13]

in Fig. 9, curves are very close to one another, and effects of scaling are predictable.

5 Enhanced shot noise in CNT-FETs

A p_z-orbital tight-binding Hamiltonian has been adopted, considering four transversal modes [28]. All simulations have been performed at room temperature, self-consistently solving the 3D Poisson and Schrödinger equations within the Non-Equilibrium Green's Functions (NEGF) formalism by means of our open-source simulator NanoTCAD ViDES [27] and considering almost 1000 statistical configurations of incoming states of the many-particle system. In order to evaluate the zero-frequency noise power spectrum $S(0)$, we have exploited the statistical approach derived in Refs. [13,14] and presented in Sect. 2, that extends Landauer–Buttiker's approach by including the effect of Coulomb interaction.

Noise current power spectral density at zero frequency $S(0)$ can be expressed as $S(0) = S_{PN}(0) + S_{IN}(0)$, where S_{PN} and S_{IN} represent the partition and the injection noise contributions, respectively.

A measure of correlation between charge carriers is the so-called Fano factor $F \equiv S(0)/(2eI) \equiv F_{PN} + F_{IN}$, where the term $2eI$ corresponds to the full shot noise spectrum, whereas $F_{PN} \equiv S_{PN}(0)/(2eI)$ and $F_{IN} = S_{IN}(0)/2eI$.

By neglecting the effect on noise of Coulomb interaction among electrons, and in particular the dependence of the transmission and reflection matrices upon the actual occupation of injected states in the device [13,14], $S(0)$ reduces to the result from Landauer [42] and Büttiker [26] $S_{LB}(0)$, that only includes the correlation among charge carriers due to their fermionic nature (Pauli exclusion principle). In a similar way, we introduce $F_{LB} \equiv S_{LB}(0)/(2eI)$.

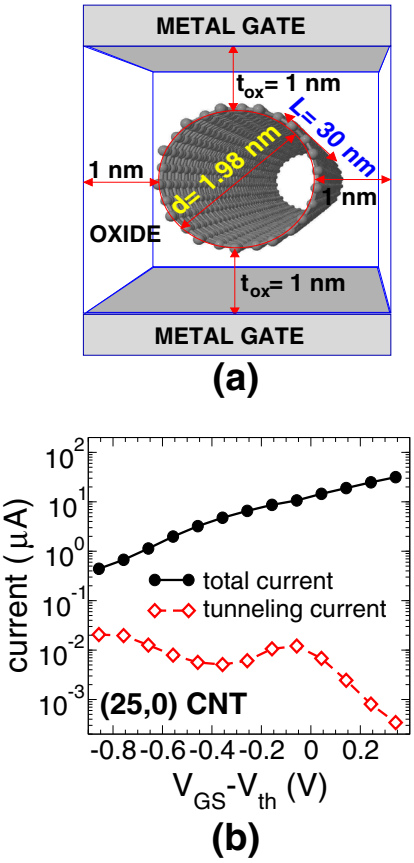

Fig. 10 **a** Sketch of the simulated (25,0) DG-CNT Field Effect Transistor. **b** Transfer characteristics and tunneling current for (25,0) CNT-FETs

The considered device is a double gate CNT-FET: the nanotube is a 2 nm diameter zig-zag (25,0) CNT with a band gap $E_g = 0.39$ eV. The oxide thickness is 1 nm, the channel is undoped and has a length L_C of 10 nm. Source (S) and Drain (D) extensions are 10 nm long and doped with a molar fraction $f = 5 \times 10^{-3}$. For comparison purposes, we also consider a (13,0) CNT-FET ($E_g = 0.75$ eV) with the same device geometry and doping profile [13,14]. In Fig. 10b the tunneling current component and the total current are reported as a function of the gate overdrive $V_{GS} - V_{th}$ for a (25,0) CNT-FET ($V_{th} = 0.36$ V). As can be observed, the tunneling component is at least two orders of magnitude smaller than the total current, which therefore is almost equal to the thermionic component.

The Fano factors for a (25,0) and a (13,0) zig-zag CNT are plotted as a function of gate overdrive in Figs. 11a-b. Noise enhancement occurs only in the case of the (25,0) CNT ($F > 1$) [20,21]. If one neglects Coulomb interaction among carriers, the Fano factor (F_{LB}) is smaller than one. *The whole shaded area in Fig.* 11a *indicates the shot noise enhancement due to the Coulomb interaction.*

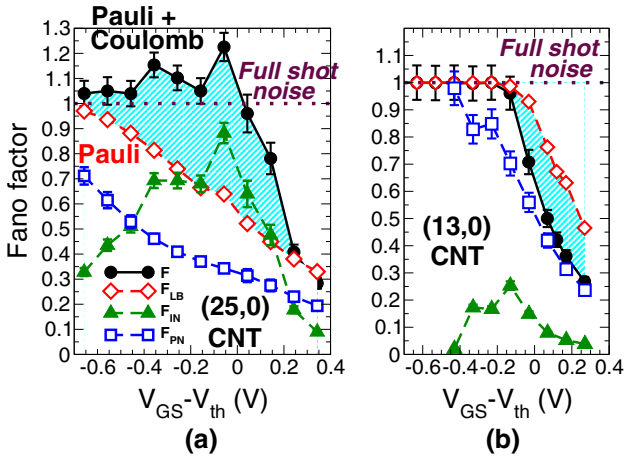

Fig. 11 Fano factor as a function of the gate overdrive for **a** (25,0) and **b** (13,0) CNT-FETs for $V_{DS} = 0.5$ V. The different contributions F_{LB}, F_{IN}, F_{PN} and the total Fano factor F are shown. From Ref. [20]

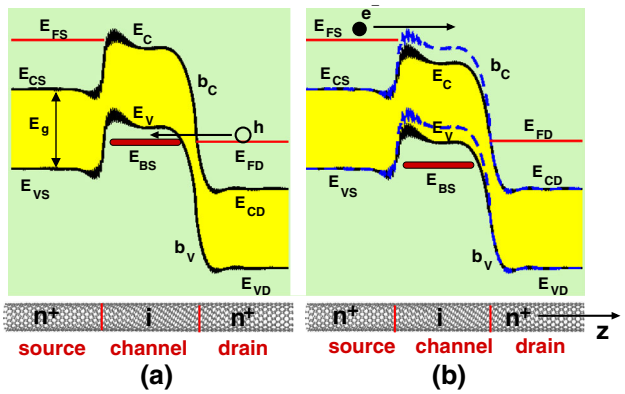

Fig. 12 If an excess hole tunnels from the drain into a bound state in the intrinsic channel (**a**), the conduction band b_C and valence band b_V edge profiles are shifted downwards and more thermionic electrons can be injected in the channel, enhancing current fluctuations (**b**). From Ref. [20]

For (13,0) CNTs, instead, Coulomb interaction suppresses noise below the value predicted by only including Pauli exclusion, as already observed in Refs. [13,14]. The different behavior is strictly associated to the different amplitude of the injection noise (F_{IN} in Fig. 1), that is much larger for (25,0) CNTs. For both CNTs, in the deep sub-threshold regime, full shot noise is obtained, since carriers are so scarce in the channel that correlations are irrelevant.

Shot noise enhancement in the (25,0) CNT-FET can be explained with the help of Fig. 12 [20,21]. E_C and E_V are the conduction and valence band edge profiles in the channel, respectively, whereas E_{CS} (E_{CD}) is the conduction band edge at the source (drain), and E_{BS} is the energy level of the quasi-bound state in the valence band. When the drain Fermi level E_{FD} roughly aligns with E_{BS}, holes in the conduction band in correspondence of the drain can tunnel into the bound state shifting downwards E_C in the channel by

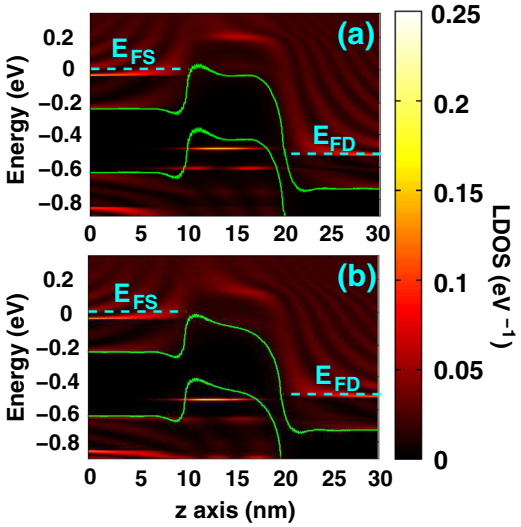

Fig. 13 Local density of states (LDOS (eV^{-1})) as a function of the longitudinal direction z for two different V_{GS}: 0 V (**a**) and 0.3 V (**b**). The bias V_{DS} is 0.5 V. Conduction band maximum E_C as a function of the number of electrons transmitted in the channel for (**a**) (25,0) and (**b**) (13,0) CNTs

$-e^2/(C_T L_C)$, where C_T is the total geometrical capacitance of the channel per unit length. As a result, thermionic electrons injected from the source can more easily overcome the barrier. Instead, when a hole leaves the bound state, the barrier increases by the same amount, reducing thermionic injection. The noise enhancement is fully due to current modulation due to trapping/detrapping of holes in the bound state.

Since (13,0) CNTs have a much wider gap ($E_g = 0.75$ eV), E_V in the channel is always below E_{CD} in the drain, and hole injection is completely inhibited, as well as noise enhancement.

The effect just illustrated resembles generation-recombination noise in semiconductors [43], since bound states in the valence band act like traps. Three remarkable differences can however be found: i) the channel in this case is defect-free, and the trap-like behavior depends on the particular bias condition; ii) the generation-recombination process in this case is associated to a spatial movement of charge (drain-channel) and is therefore similar to what observed in Refs. [8,9] for MOS capacitors; iii) in classical generation-recombination noise current fluctuations are due to fluctuations of the number of charge carriers, whereas here transport is elastic and current fluctuations are due to fluctuations in the occupation of injected states for electrons and holes and to the induced fluctuations of the potential barrier.

To justify our assertion, let us focus on the local density of states (LDOS) computed for the (25,0) CNT. In Figs. 13a-b the LDOS averaged on each carbon ring is shown as a function of the coordinate along the transport direction z for two gate voltages in correspondence of the peaks in

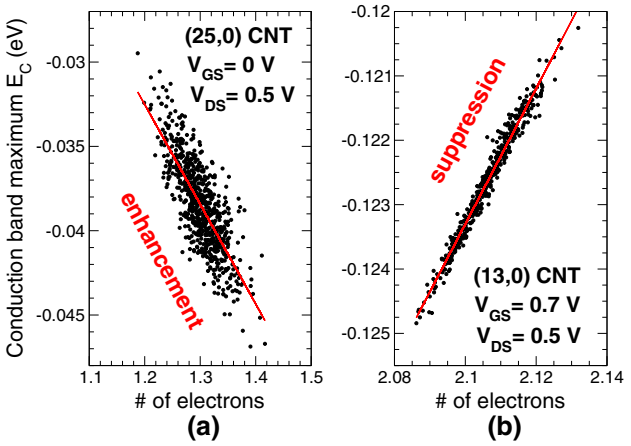

Fig. 14 Conduction band maximum E_C as a function of the number of electrons transmitted in the channel for **a** (25,0) and **b** (13,0) CNTs. From Ref. [20]

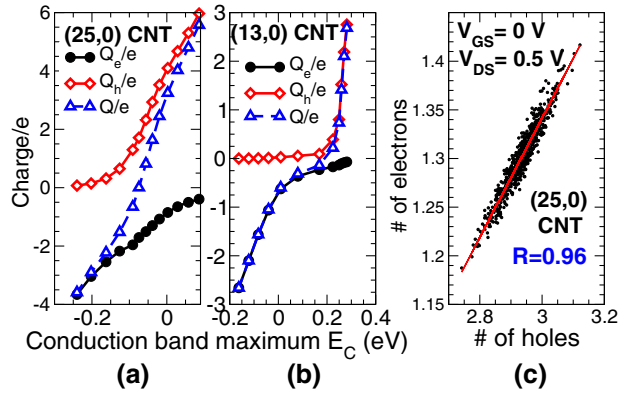

Fig. 15 Electron, hole and total charge as a function of E_C for **a** (25,0) and **b** (13,0) CNTs. **c** Number of electrons transmitted in the channel as a function of the number of holes tunneling from the drain

Fig. 11a, i.e. $V_{GS} = 0$ V and 0.3 V, and a drain-to-source bias $V_{DS} = 0.5$ V: two localized states appear in the valence band, due to the local confinement. Since the energy of the highest quasi-bound state is close to the drain Fermi energy, hole tunneling in and out of the channel can occur, with a zero net current flow. As shown in Fig. 11a, shot noise enhancement ($F = 1.22$) is observed whenever the applied gate voltage roughly aligns E_{BS} with E_{FD}, i.e. in the range $-0.4\,\text{V} < V_{GS} - V_{th} < 0.1\,\text{V}$.

In Figs. 14 and 15, we show the scatter plots obtained from Monte Carlo simulations. In particular, Figs. 14a-b show E_C as a function of the number of injected thermionic electrons for $V_{DS} = 0.5$ V and $V_{GS} = 0.7$ V for (13,0) CNTs ($F = 0.27$) and 0 V for (25,0) CNTs ($F = 1.15$). As can be noted in Fig. 14a, the net result of an electron entering the channel of the (25,0) CNT is a decrease of the conduction band in the channel, that is at first counterintuitive, and opposite to the trend observed in (13,0) CNTs [13,14] (Fig. 14b). The different behavior is not due to a different

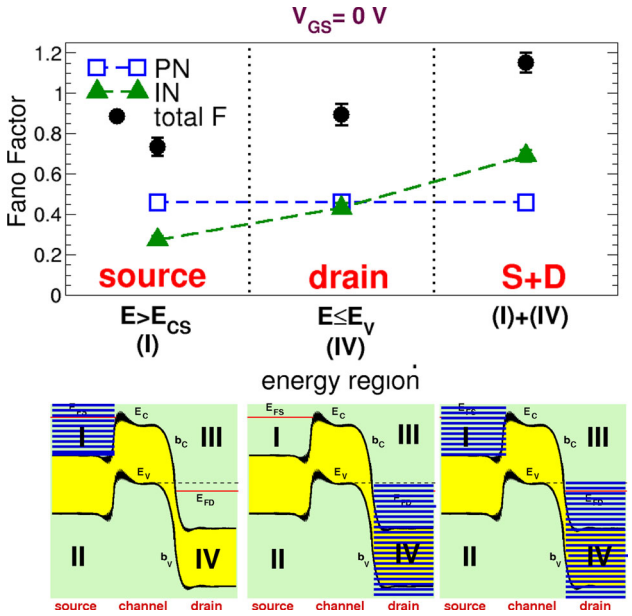

Fig. 16 F, F_{PN} and F_{IN} when randomizing the occupancy at different energy regions and at different reservoirs (source (S): I,II; drain (D): III, IV) for $V_{GS} = 0$ V. *Shaded areas* indicate energy regions where the occupancy is randomized

screening of the gate field, since the quantum capacitance in the channel $e\,\partial Q/\partial E_C$ (Q is the net charge in the channel) is expected to be positive in both cases (Figs. 15a-b). However, it is fully consistent with the interpretation proposed above for the noise enhancement in (25,0) CNT. Actually, the apparently strange behavior of Fig. 14a is due to the positive correlation between holes in the quasi-bound state and thermionic electrons. This is further confirmed by Fig. 15c, which highlights a strong correlation between statistical fluctuations of holes and electrons in the channel, as proved by the almost unity correlation factor ($R = 0.96$). In addition the slope of the line is close to 0.5, which means that for every two holes that are injected in the channel, electron count in the channel roughly increases by one. To highlight the correlation between electrons and holes we can divide the states injected from the reservoirs in 4 regions: regions I ($E > E_{CS}$) and II ($E \leq E_{CS}$) refer to source injected states, whereas regions III ($E > E_V$) and IV ($E \leq E_V$) to drain injected states. Regions II and III of course do not contribute neither to transport, nor to charge fluctuations. Instead turning on random injection of states only for region I or IV, the enhancement disappears (Fig. 16), pointing out that the positive correlation between hole interband tunneling from the drain and thermionic electron injection from the source is key to enhancement. In addition, the total injection noise obtained by randomizing the statistics everywhere can be roughly expressed as the sum of the injection noise contributions obtained by separately randomizing the statistics in regions I and IV. Partition noise is instead not affected by the

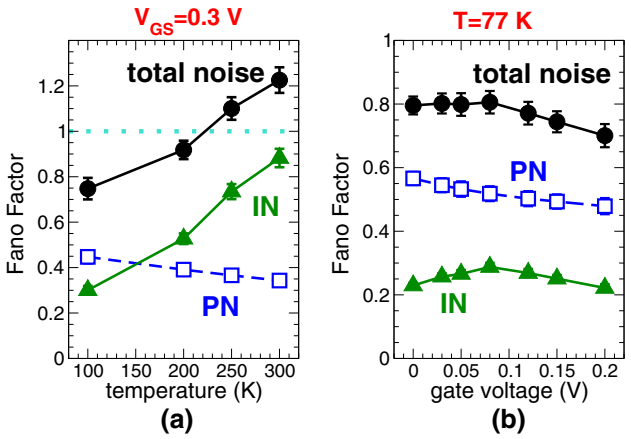

Fig. 17 **a** F, F_{PN} and F_{IN} at $V_{GS} = 0.3$ V as a function of temperature and **b** as a function of V_{GS} for T = 77 K

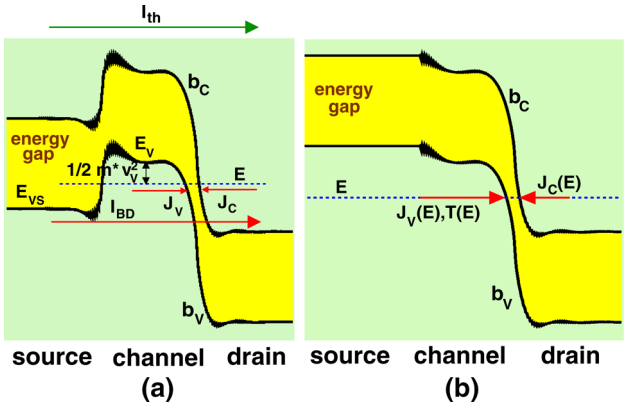

Fig. 18 **a** Conduction and valence band edge profiles for $V_{DS} = 0.5$ V and $V_{GS} = 0$ V. **b** Band profile used to evaluate the transmission coefficient $T(E)$

considered statistics (Fig. 16), because it is fully taken into account by the shot noise formula [13,14].

Significantly, lowering the temperature (Fig. 17a) suppresses shot noise enhancement by reducing the injection noise, due to the suppression of the hole trapping-detrapping process. Therefore, at T=77 K (Fig. 17b) noise enhancement disappears, although a maximum in the injection noise can still be observed when E_{BS} almost aligns with E_{FD}. It is also interesting to evaluate the cutoff frequency f_H of shot noise enhancement, which in this case is limited by the process of charging and discharging channel with holes: it is therefore the cutoff frequency of an R-C circuit, where C is the total capacitance of the channel, and R is the quasi-equilibrium resistance between drain and channel [20,21]. In order to do that, we need to evaluate C from Fig. 15a, obtaining $C \approx 5.5$ aF.

Then we need to compute the conductance $G = 1/R$ between the channel and the drain due to interband tunneling. Following Bardeen [44], tunneling can be treated as an electronic transition between energy levels in different regions. The matrix element for a transition at energy E from a state in the conduction band b_C at the drain into a state in the valence band b_V in the channel can be expressed as [45]:

$$M(E) = \hbar^2 T(E) J_V(E) J_C(E) \tag{8}$$

where $J_V(E)$ ($J_C(E)$) is the current probability incident on the barrier from S (D) (Fig. 18a), while $T(E)$ is the transmission probability of the interband barrier, which has been evaluated by considering the band profile in correspondence of the source constant and equal to the value assumed at source/channel interface (Fig. 18b), as in Ref. [46].

The transition probability per unit time is given by the Fermi's golden rule:

$$\nu(E) = \frac{2\pi}{\hbar} |M(E)|^2 \rho_V(E) \tag{9}$$

where $\rho_V(E)$ is the density of states in b_V in the channel. The tunneling frequency g can be obtained by summing on all empty states in b_C at the drain and on all occupied states in b_V in the channel:

$$g = 4\pi\hbar \int_{E_{VS}}^{E_V} dE\, T(E) J_V(E) J_C(E) \rho_V(E) \rho_C(E) f_D(E) \times (1 - f_D(E)), \tag{10}$$

where $\rho_C(E)$ is the density of states in b_C at the drain and the occupancy in b_V in the channel has been approximated to $f_D(E)$. By exploiting $J_C(E)\rho_C(E) = 2\pi\hbar$ [8,45], we finally obtain G as:

$$G = \left(\frac{q^2}{KT}\right) g\,. \tag{11}$$

In addition, the product $J_V(E)\rho_V(E)$ has been approximated as

$$J_V(E)\rho_V(E) \approx \frac{v_V(z_{middle}, E)}{2\,L_C} \int_{channel} \rho_V(z, E) dz, \tag{12}$$

where L_C is the channel length, $v_V(z_{middle}, E)$ is the velocity of a carrier with energy E coming from the left and computed at the longitudinal coordinate z_{middle} (in the middle of the channel), whereas $\rho_V(z, E)$ is the mean DOS computed at E and z. $v_V(z, E)/(2L_C)$ instead represents the attempt frequency in the device region [45].

Instead the electron velocity can be derived through the effective mass approximation. The effective mass for a CNT [47] reads $m^* = \left(4\hbar^2\right) / \left(9 a_{CC} d t_0\right)$, where $a_{CC} = 0.144$ nm is the carbon-carbon (CC) bond length, $t_0 = 2.7$ eV is the nearest neighbor CC tight binding overlap energy, $d = 1.98$ nm is the diameter of the carbon nanotube. The kinetic energy $1/2\, m^* v_V(z, E)^2$ is instead given by the difference between the valence band edge in the channel at the longitudinal coordinate z and the total energy E (see Fig. 18a). We obtain $G \approx 4.7 \times 10^{-5}$ S. Note that G and C are such

that we are at the limit of the Coulomb blockade regime: the charging energy is comparable to the thermal energy, but we can still consider $f_H = G/(2\pi C) \approx 1.36$ THz.

6 Concluding remarks

In this paper we have reviewed simulations of shot noise in ballistic quasi one-dimensional CNT-FETs and SNW-FETs by self-consistently solving the electrostatics and the transport equations within the NEGF formalism, within a recently proposed statistical approach which manages to include also Coulomb repulsion among electrons. We have shown that both suppression and enhancement of shot noise can be observed, and have invited experimental groups to the challenge.

First, we have focused on (13,0) CNT-FETs and SNW-FETs, obtaining a shot noise suppression. In particular, we have shown that by only using Landauer–Büttiker noise formula, i.e. considering only Pauli exclusion principle, one can overestimate shot noise by as much as 180 %. Furthermore, with our approach we are able to observe a rectification of the DC characteristics due to fluctuations of the channel potential, and to identify and evaluate quantitatively the different contributions to shot noise. We are also able to consider the exchange interference effects, which are often negligible but can be measurable when a defect, introducing significant mode mixing, is inserted in the channel.

Then, we have shown that shot noise enhancement can be observed in (25,0) CNT-FETs biased in the weak subthreshold regime, due to the modulation of thermionic current caused by interband tunneling of holes between the drain and the channel. In (25,0) CNT-FETs, the enhancement is expected to be observable down to a temperature of 200 K and at frequencies well above those in which flicker noise is dominant.

References

1. Landauer, R.: Condensed-matter physics: the noise is the signal. Nature **392**, 658–659 (1998)
2. González, T., González, C., Mateos, J., Pardo, D., Reggiani, L., Bulashenko, O.M., Rubi', J.M.: Universality of the 1/3 shot-noise suppression factor in nondegenerate diffusive conductors. Phys. Rev. Lett. **80**, 2901–2904 (1998)
3. Sukhorukov, E.V., Loss, D.: Universality of shot noise in multiterminal diffusive conductors. Phys. Rev. Lett. **80**, 4959–4962 (1998)
4. Blanter, Y.M., Büttiker, M.: Shot-noise current-current correlations in multiterminal diffusive conductors. Phys. Rev. B **56**, 2127–2136 (1997)
5. Steinbach, A.H., Martinis, J.M., Devoret, M.H.: Observation of hot-electron shot noise in a metallic resistor. Phys. Rev. Lett. **76**, 3806–3809 (1996)
6. Schoelkopf, R.J., Burke, P.J., Kozhevnikov, A.A., Prober, D.E., Rooks, M.J.: Frequency dependence of shot noise in a diffusive mesoscopic conductor. Phys. Rev. Lett. **78**, 3370–3373 (1997)
7. Iannaccone, G.: Analytical and numerical investigation of noise in nanoscale ballistic field effect transistors. J. Comput. Electron. **3**, 199–202 (2004)
8. Iannaccone, G., Crupi, F., Neri, B.: Suppressed shot noise in trap-assisted tunneling of metal-oxide-semiconductor capacitors. Appl. Phys. Lett. **77**, 2876–2878 (2000)
9. Iannaccone, G., Crupi, F., Neri, B., Lombardo, S.: Theory and experiment of suppressed shot noise in stress-induced leakage currents. IEEE Trans. Electron Dev. **50**, 1363–1369 (2003)
10. Carlo, L.D., Williams, J.R., Zhang, Y., McClure, D.T., Marcus, C.M.: Shot noise in graphene. Phys. Rev. Lett. **100**, 156801 (2008)
11. Herrmann, L.G., Delattre, T., Morfin, P., Berroir, J.M., Placais, B., Glattli, D.C., Kontos, T.: Shot noise in fabry-perot interferometers based on carbon nanotubes. Phys. Rev. Lett. **99**, 156804 (2007)
12. Betti, A., Fiori, G., Iannaccone, G.: Shot noise in quasi one-dimensional FETs. IEDM Technol. Digest 185–188 (2008)
13. Betti, A., Fiori, G., Iannaccone, G.: Shot noise suppression in quasi one-dimensional field effect transistors. IEEE Trans. Electron Dev. **56**, 2137–2143 (2009)
14. Betti, A., Fiori, G., Iannaccone, G.: Statistical theory of shot noise in quasi-1D field effect transistors in the presence of electron–electron interaction. Phys. Rev. B **81**, 035329 (2010)
15. Iannaccone, G., Lombardi, G., Macucci, M., Pellegrini, B.: Enhanced shot noise in resonant tunneling: theory end experiment. Phys. Rev. Lett. **80**, 1054 (1998)
16. Iannaccone, G., Macucci, M., Pellegrini, B.: Shot noise in resonant-tunneling structures. Phys. Rev. B **55**, 4539–4550 (1997)
17. Pedersen, M.B.M.H., van Langen, S.A., Büttiker, M.: Charge fluctuations in quantum point contacts and chaotic cavities in the presence of transport. Phys. Rev. B **57**, 1838 (1998)
18. Büttiker, A.P.M., Thomas, H., Prêtre, A.: Dynamic conductance and the scattering matrix of small conductors. Phys. Lett. A **180**, 364 (1993)
19. Betti, A., Fiori, G., Iannaccone, G.: Shot noise analysis in quasi one-dimensional field effect transistors. Int. Conf. Noise Fluct. **1129**, 581–584 (2009)
20. Betti, A., Fiori, G., Iannaccone, G.: Enhanced shot noise in carbon nanotube field-effect transistors. Appl. Phys. Lett. **95**, 252108 (2009)
21. Betti, A., Fiori, G., Iannaccone, G.: Enhanced shot noise in carbon nanotube FETs due to electron–hole interaction. IWCE Technol. Dig. 1–4 (2010)
22. Datta, S.: Electronic Transport in Mesoscopic Systems. Cambridge University Press, Cambridge (1995)
23. Landauer, R.: Spatial variation of currents and fields due to localized scatterers in metallic conduction. IBM J. Res. Dev. **1**, 223 (1957)
24. Sai, N., Zwolak, M., Vignale, G., Di Ventra, M.: Dynamical corrections to the DFT–LDA electron conductance in nanoscale systems. Phys. Rev. Lett. **94**, 186810 (2005)
25. Vignale, G., Di Ventra, M.: Incompleteness of the Landauer formula for electronic transport. Phys. Rev. B **79**, 014201 (2009)
26. Büttiker, M.: Scattering theory of current and intensity noise correlations in conductors and wave guides. Phys. Rev. B **46**, 12485–12507 (1992)
27. Code and documentation can be found at the url: http://www.nanohub.org/tools/vides
28. Fiori, G., Iannaccone, G.: Coupled mode space approach for the simulation of realistic carbon nanotube field-effect transistors. IEEE Trans. Nanotechnol. **6**, 475 (2007)
29. Guo, J., Datta, S., Lundstrom, M., Anantam, M.P.: Towards multi-scale modeling of carbon nanotube transistors. Int. J. Multiscale Comput. Eng. **2**, 257–276 (2004)
30. Fiori, G., Iannaccone, G.: Three-dimensional simulation of one-dimensional transport in silicon nanowire transistors. IEEE Trans. Nanotechnol. **6**, 524–529 (2007)

31. Wang, J., Polizzi, E., Lundstrom, M.: A three-dimensional quantum simulation of silicon nanowire transistors with the effective-mass approximation. J. Appl. Phys. **96**, 2192–2203 (2004)
32. Fiori, G., Iannaccone, G., Klimeck, G.: A three-dimensional simulation study of the performance of carbon nanotube field-effect transistors with doped reservoirs and realistic geometry. IEEE Trans. Electron Dev. **53**, 1782–1788 (2006)
33. Park, H.H., Jin, S., Park, Y.J., Min, H.S.: Quantum simulation of noise in silicon nanowire transistors. J. Appl. Phys. **104**, 023708 (2008)
34. Gramespacher, T., Büttiker, M.: Local densities, distribution functions, and wave-function correlations for spatially resolved shot noise at nanocontacts. Phys. Rev. B **60**, 2375–2390 (1999)
35. Büttiker, M.: Flux-sensitive correlations of mutually incoherent quantum channels. Phys. Rev. Lett. **68**, 843–846 (1992)
36. Park, H.H., Jin, S., Park, Y.J., Min, H.S.: Quantum simulation of noise in silicon nanowire transistors with electron–phonon interactions. J. Appl. Phys. **105**, 023712 (2009)
37. van der Ziel, A.: Noise in Solid State Device and Circuits, pp. 75–78. Wiley, New York (1986)
38. Abidi, A.A.: High-frequency noise measurements on FET's with small dimensions. IEEE Trans. Electron Dev. **33**, 1801–1805 (1986)
39. Navid, R., Dutton, R.W.: The physical phenomena responsible for excess noise in short-channel MOS devices. IEDM Technol. Dig. 75–78 (2002)
40. Han, K., Shin, H., Lee, K.: Analytical drain thermal noise current model valid for deep submicron MOSFETs. IEEE Trans. Electron Dev. **51**, 261–269 (2004)
41. Bulashenko, O.M., Rubí, J.M.: Shot-noise suppression by Fermi and Coulomb correlations in ballistic conductors. Phys. Rev. B **64**, 045307 (2001)
42. Martin, T., Landauer, R.: Wave-packet approach to noise in multichannel mesoscopic systems. Phys. Rev. B **45**, 1742–1755 (1992)
43. Döring, M.R., Hangleiter, A., Klötzer, N.: Electron–hole correlation effects in generation–recombination noise. Phys. Rev. B **45**, 1163–1171 (1992)
44. Bardeen, J.: Tunneling from a many-particle point of view. Phys. Rev. Lett. **6**, 57–59 (1961)
45. Iannaccone, G., Pellegrini, B.: Unified approach to electron transport in double-barrier structures. Phys. Rev. B **52**, 17406–17412 (1995)
46. Reittu, H.J.: Fermi's golden rule and Bardeen's tunneling theory. Am. J. Phys. **63**, 940–944 (1995)
47. Ahmadi, M.T., Ismail, R., Tan, M.L.P., Arora, V.K.: The ultimate ballistic drift velocity in carbon nanotubes. J. Nanomater. **2008**, 769250 (2008)